Corrosion Behavior Characterization of the Nugget Zone in Copper/Brass Metals of Dissimilar Friction Stir Welded Lap Joints

Kamran Amini*
Young Researchers and Elite Club, Tiran Branch,
Islamic Azad University, Isfahan, Iran
E-mail: k_amini@iautiran.ac.ir
*corresponding author

Farhad Gharavi
Department of Materials Engineering,
Sirjan Branch, Islamic Azad University, Sirjan, Iran
E-mail: fgharavi@iausirjan.ac.ir

Received: 18 October 2017, Revised: 28 November 2017, Accepted: 17 December 2017

Abstract: The electrochemical behavior of the weld nugget zone (WNZ) in copper-brass plates was studied in this paper. These plates were welded by the friction stir lap welding method in 1M NaCl solution at low heating input (450 rpm-25 mm/min) and high heating input (710 rpm-16 mm/min) by using the electrochemical impedance spectroscopy (EIS) and Tafel polarization at ambient temperature. The morphology of nugget zone corroded surfaces was analyzed by SEM (scanning electron microscopy) technique. The welding process appeared to decrease the corrosion resistance of the welded nugget regions through increasing the welding heat input. The results from EIS measurements presented the welded joints of NZ which showed higher and lower values respectively than brass and copper. Due to changing of microstructural of weld nugget zone during welding process, the I_{corr} of nugget zone enhances with increasing welding heat input. In fact, the surface corrosion morphology analysis revealed that the surface of welded sample by high heating input was shielded with a roughly porous corrosion layer rather than the surface of the welded sample at low heating input.

Keywords: Brass, Copper, Electrochemical behavior, Friction stir welding, Lap joint

Reference: Kamran Amini, and Farhad Gharavi, "Corrosion Behavior Characterization of the Nugget Zone in Copper/Brass Metals of Dissimilar Friction Stir Welded Lap Joints", Int J of Advanced Design and Manufacturing Technology, Vol. 11/No. 1, 2018, pp. 97-104.

Biographical notes: K. Amini received his PhD in Materials Eng., from University of IAU, Science and Research Branch, in 2010. He is currently associated professor at the Department of Mechanical Eng., Tiran Branch, Islamic Azad University, Isfahan, Iran. His current research interest includes Heat Treatment Processes, and Surface Engineering. **F. Gharavi** received his PhD in Advanced Materials Eng., from University of Putra Malaysia (UPM), in 2014. He is currently Assistant professor at the Department of Materials Eng., Sirjan Branch, Islamic Azad University, Sirjan, Iran. His current research interest includes Friction Stir Welding & Processing, and Corrosion Engineering.

1 INTRODUCTION

Due to their outstanding thermal and electrical conductivity properties associated with corrosion resistance feature, copper and its alloys are widely used in various industrial areas, particularly in marine uses, outdoor constructions such as roofs, facades and cladding [1]. Brass, an important copper alloy, involves an extensive range of applications, including material tubing for heat exchangers and condensers in many cooling water systems [2]. Joining of dissimilar alloys is a necessary process in several industrial applications, which requires understanding the welding processes and their impacts on the corrosion properties.

In fact, joining copper and brass by conventional fusion welding method may face some difficulties due to events such as cracks, severe deformation, porosities, high residual stress, and evaporation of alloying elements, particularly the zinc [3]- [4].

The friction stir welding (FSW) is a new solid-state joining process that was invented in 1991, which can prevent many difficulties related to the fusion welding processes. As a result, we will be able to produce defect-free welds with suitable properties even in materials with poor fusion weld ability [5]-[6]. Numerous advantages of FSW have drawn the attention of various industries. The method is efficiently used in joining the copper and its alloys to prevent the evaporation of alloy elements and provide high heat input required for fast heat radiation as well as minimize the strength loss in the welding region [4]-[6].

In practice, all the structures with welded joints are exposed to numerous aggressive environments throughout their service life. The environmental media play a major role in the durability of welded structural materials. Moreover, different corrosion media may affect the corrosion characteristics of welded structure via varying PHs and chemical compositions, which can effectively simulate the actual marine environment [7]-[9]. Although copper and its alloys are resistant to corrosion, they may corrode in the solutions containing chloride, oxygen, sulphide, sulphate, and nitrate ions [9].

The corrosion resistance rates of friction stir welded materials occurring at various regions during the welding process are not similar due to clear microstructure gradient caused by the plastic deformation and storage heating effect during the FSW process. Therefore, the FSW impact on the corrosion behavior of copper and its alloys has hardly regarded.

In current studies, it was suggested that the FSW process of copper and brass metals might happen in an aqueous chloride medium. The corrosion resistance of the weld nugget zone has been examined in the FSW of Cu-brass plates in a 1M NaCl solution using electrochemical impedance spectroscopy (EIS) and Tafel polarization. Furthermore, the optical microscopy and scanning electron microscopy were used to investigate the effect of this welding method on the welded joint microstructure and evaluate the corroded surface of the weld nugget region.

2 EXPERIMENTAL METHOD

The materials used in this study included 5 mm brass plates and pure copper plates. The compositions are shown in Tables 1 and 2. Before the start of welding, the 220 × 140 × 5 mm^3 plates were cut and prepared in distilled water ad anhydrous alcohol. Then, the friction stir welding process was done on different alloys, copper and brass in the lap weld configuration by using a CNC Machine.

Figure 1 illustrates the schematic representation of the welding process and the joint design. In the joint design, the plates of brass and copper were placed in Advancing and Retreating sides, respectively. Table 3 provides a list of the tool's size. The shape geometry of welding tool is provided in Fig. 2. The welding direction 200 mm in length was parallel to the rolling direction. A left-hand threaded conical probe and concave shoulder characterized the welding tool. The dimensions of the tool welding are shown in Table 3. Through the welding process, the stir tool was held in the clockwise direction, tilted as 2°. The tool shoulder plunging depth was 0.2 mm. All welded samples were welded at two welding heat inputs, denoted as FSLW1 with a low heat input (450 rpm-25 mm/min) and FSLW2 with a high heat input (710 rpm-16 mm/min).

Table 1 The copper plate chemical composition (mass %)

Element	Cu	Sn	Ni	Si	Ag
Min.	99.93	0.024	0.013	0.005	0.024

Table 2 The brass plate chemical composition (mass %)

Element	Cu	Zn	Fe	Ni	Si	P	Pb
Min.	62.43	37.21	0.15	<0.001	<0.001	0.01	0.08

Table 3 Tool Size used in the experiment

Length of pin (mm)	Diameter of pin (mm)	Diameter of shoulder (mm)	Pitch (mm)	Cone Angle (degree)
9.50	10.50	24	1.2	60

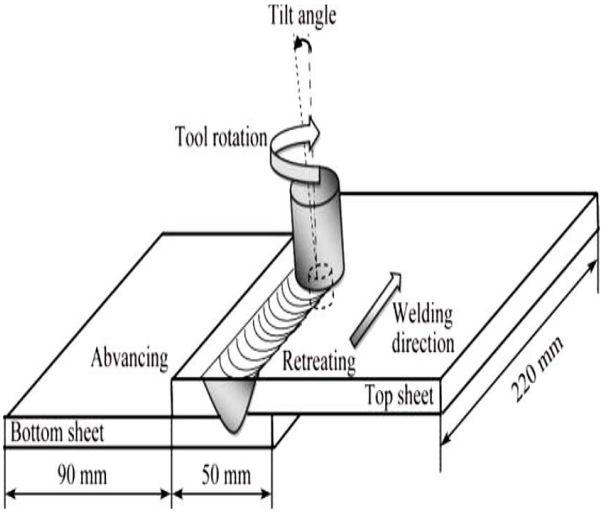

Fig. 1 A schematic of the friction stir lap welding process and the joint design used in the study

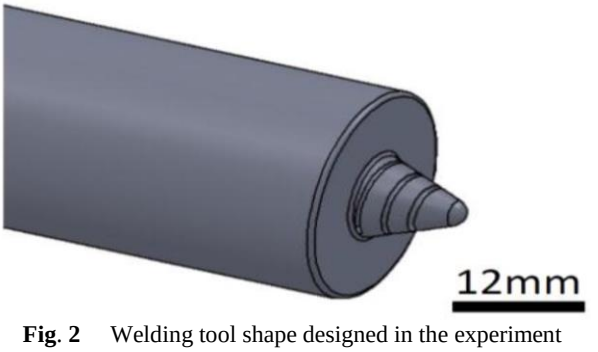

Fig. 2 Welding tool shape designed in the experiment

Electrochemical measurements were made using a three-electrode method through exposing to a 1M NaCl solution under an ambient temperature. Among the welding settings, the NZ samples were selected as the working electrodes (WE), a graphite rode was used as the counter electrode (CE), while a saturated calomel electrode (SCE) was chosen to be the reference electrode (RE). First, an open circuit potential (OCP) was documented in a three-electrode cell. Then, a steady state OCP was obtained after 1 h of immersion in the test solution. Subsequently, an electrochemical impedance spectroscopy (EIS) was performed with a voltage amplitude of ±10 mv in a frequency range of 0.01 to 100 kHz. Then, the Tafel polarization curves were schemed through starting the scanning electrode potential of -0.25 to +1.1 V versus OCP at 1 mv/s scan rate.

All the samples were ground with abrasive papers up to 1500 grit before the tests, and then polished using a 1µ diamond paste. Finally, using acetone, they were cleaned. An optical microscope (OM) examined the morphologies of transverse cross-section in the weld nugget zones examined by the end of polishing and etching with Keller's reagent. Using a scanning electron microscope (SEM), the morphology of the corrosion surface was evaluated.

3 RESULTS AND DISCUSSION

3.1 OPEN CIRCUIT POTENTIAL (OCP) ASSESSMENTS

Figure 3 shows the E_{ocp} data measured for the base materials (BM), pure copper and brass; it also presents two nugget zones for the welded copper/brass metals by FSLW after immersion in the as-prepared 1M NaCl solution (pH 7.2) for 3600s.

As seen, the E_{ocp} gets more negative over time in all the specimens. The E_{ocp} curves reduced upon sample immersion before reaching to the steady state value. The decrease in E_{ocp} is resulted from the oxide film breakdown on the surface of all samples. Moreover, in keeping with Fig. 3, one can see that the steady state E_{ocp} of Cu, brass, and welded samples nugget zones were displaced marginally.

In addition, it was reached after 1000s. It also demonstrates that the brass sample has the lowest E_{ocp}, which is due to the occurrence of Zn dealloying or the phenomenon of dezincification on the brass sample surface. Some believe that the de-alloying significantly depends on the differences between atomic composition, the standard reversible potentials of major constituent elements, and the kinetics of the diffusion of alloyed elements solid state [10]- [11].

According to E-pH diagrams of Fig. 4, the dealloying of brass metal is neutral to lower pH solution due to selective dissolution of Zn. Based on Figure 4, one can realize that the welded samples nugget zone is less susceptible to the dealloying in the NaCl than the Cu-Zn alloy.

Furthermore, the E_{ocp} is decreased by increased heat input during the welding process, showing the lowest and highest values compared with the pure copper and brass metals, respectively. Therefore, the welded samples of the nugget zones show higher tendency to the Zn dealloying phenomenon, while the corrosion of welded samples increases by heat input during the welding process. Consequently, the heat input can change the microstructure of the welded samples of the nugget zone during the welding process, and thus, the microstructural aspects may intensely affect the stability and the nature of formed oxide film on the welded samples surface.

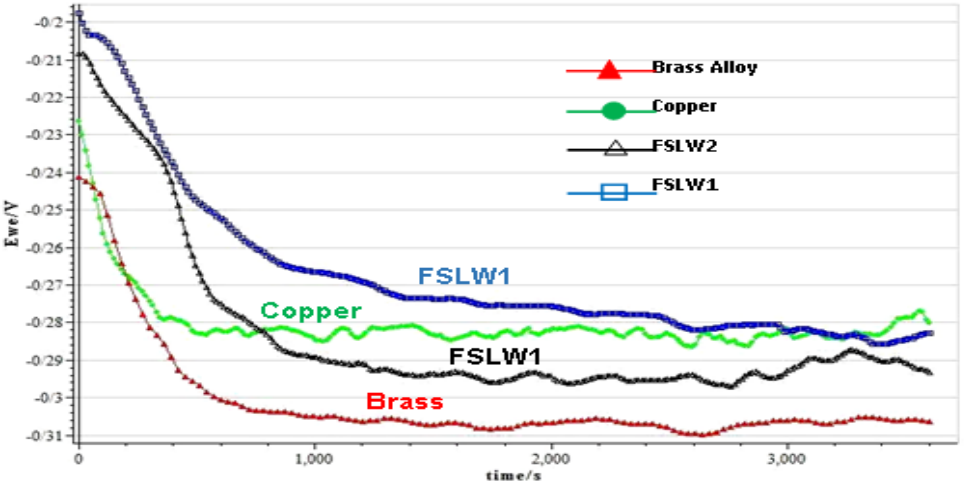

Fig. 3 Open circuit measurements for Cu, brass alloy and welded copper/brass nugget zones in M NaCl (pH 702) for 1 h

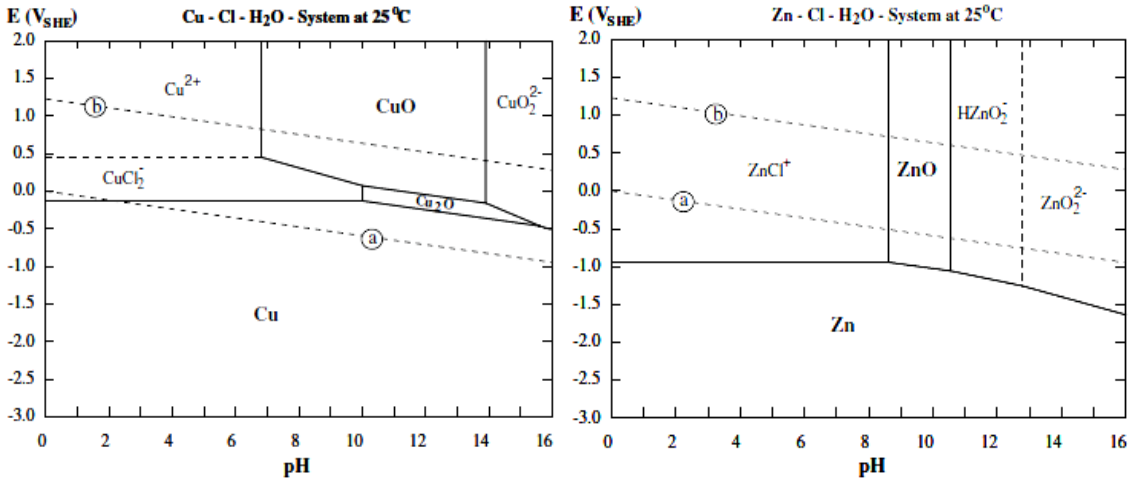

Fig. 2 Pourbaix diagrams (E-pH) of pure Cu and Zn (Cl – H2o system at 25℃with 0.67 activity of Cl) equivalent to 1 M NaCl

3.2 POLARIZATION BEHAVIOR

Figure 5 demonstrates the potentio-dynamic polarization behavior of all samples in near neutral (pH. 7.2) 1M NaCl solution following the immersion for 3600s.

As seen, all samples exhibit the same curve shape, where the current varies smoothly and linearly around the rest of the potential, showing cathodic and anodic Tafel behavior. However, in case of brass alloy, the E_{ocp} was around -0.28V_{SCE}, which is marginally less than the others. Table 4 represents the corrosion potential (E_{corr}), corrosion current density (I_{corr}), and corrosion rate (mpy). Using Tafel extrapolation of the linear part of the cathodic branch, the corrosion current density (I_{corr}) was calculated with an accuracy of more than 95% for the points more negative to E_{corr} by 50mv [12]. With increased heat input, the I_{corr} of the nugget zones increases due to the intrinsic microstructural changes happening during the FSLW process. This indicates that the FSW process can reduce the corrosion resistance of the welded copper/brass metals. As it can be seen in Fig. 5, the curves anodic branches can be divided into two potential areas. The first region is the Tafel behavior area where the reaction has to be fully limited by the charge transfer. Within this region, we can see a rapid increase of current with potential, while both Zn and Cu are dissolved simultaneously.

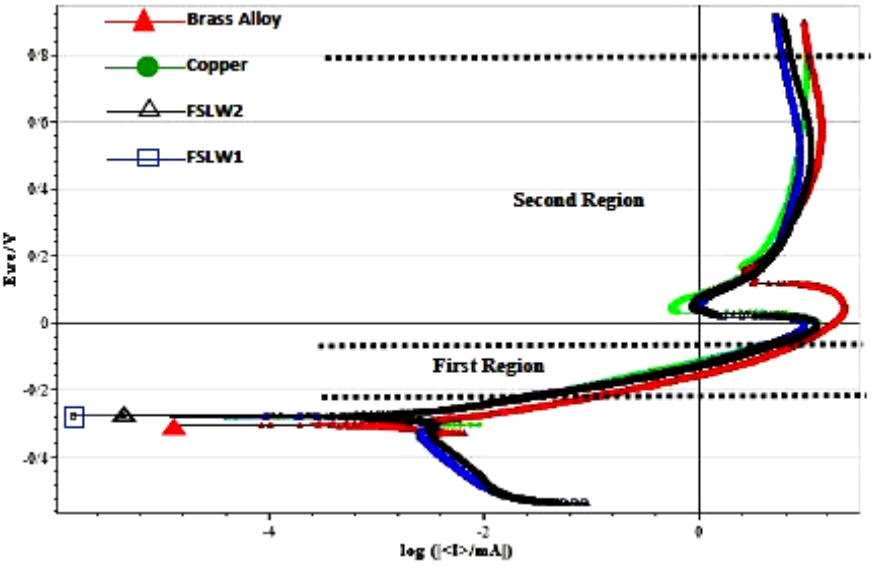

Fig.5 Polarization behavior of Cu, brass alloy and welded copper/brass nugget zone in 1 M NaCl (Ph 7.2), the arrows indicate the position of peaks II and I

Table 4 The electrochemical data derived from measurements of polarization and impedance for Cu, brass alloy and welded copper/brass nugget zone in 1 M NaCl (Ph 7.2)

Sample	E_{corr} (V/SCE)	I_{corr} (μAcm−2)	C.R (mpy)	$R_{pass} \times 10^3$ (ohm)	$R_{ct} \times 10^3$ (ohm)	$R_{pol} \times 10^3$ (ohm)
Cu	-0.284	3.34	1.53	21.61	0.036	21.65
Brass	-0.303	6.76	3.11	10.11	0.075	10.18
FSLW1	-0.279	4.19	1.92	19.75	0.029	19.81
FSLW2	-0.276	5.37	2.46	20.62	0.059	20.68

As Zn dissolves according to Eq. (1), according to the pourbaix diagram (Fig. 4) prediction, the Cu dissolves based on reactions (2) and (3) at moderate and high potentials, respectively [10]:

$$Zn \longrightarrow Zn^{+2} + 2e^- \quad (1)$$

$$2Cu + H_2O \longrightarrow Cu_2O + 2H^+ + 2e^- \quad (2)$$

$$Cu_2O + H_2O \longrightarrow 2CuO + 2H^+ + 2e^- \quad (3)$$

In this region, the alloy behavior is strongly affected by the presence of chloride ions. The second region is a potential window of film formation, leading to a maximum peak current density, which subsequently will limit the current density.

The responses of maximum peak, minimum and limiting current density are more rapid than the mass transport of either its complex ion by chloride ion or the cuprous dichloride complex ($CuCl_2^-$) into the bulk solution. Therefore, the maximum peak current is followed by a minimum current meanwhile the CuCl surface coverage reaches its maximum [13]. Therefore, the anodic reaction undergoes mixed kinetics (charge transfer and mass transport) near the corrosion potential, where the mass transport-limiting step is the movement rate of a cuprous chloride complex away from the electrode surface to the bulk electrolyte.

Figure 6 schemes the variation of the corrosion current density of all samples. The pure copper sample has the I_{corr} minimum, while the brass alloy records a maximum value.

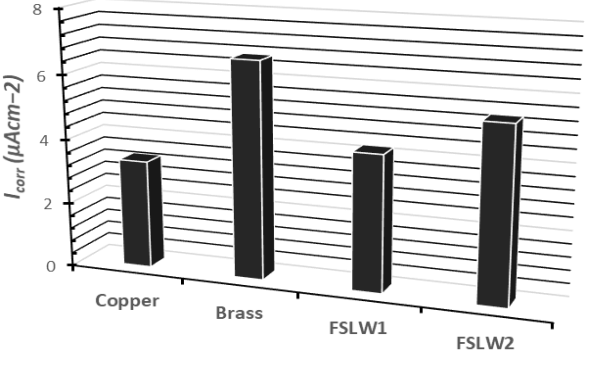

Fig. 6 The values of corrosion current density derived from potentiodynamic polarization curves for Cu, brass and weld nugget regions through FSW

Several researchers [14]-[16] have previously found that the polarization Tafel region is not activation-controlled, but it is a mass transport-kinetics process, where the diffusion rate of ($CuCl_2^-$) species from the electrode surface across a diffusion layer which controls the dissolution. The electrode potential defines its concentration gradient. Furthermore, according to Table 4, the welding process has no significant and negative effect on the corrosion potential values.

3.3 EIS MEASUREMENTS

Figure 7 shows the EIS response of all specimens through FSW after immersing for 3600s in the near neutral (pH. 7.2) 1M NaCl solution. The outcomes are shown as Nyquist and Bode plots. All the Nyquist plots display imperfect semicircles.

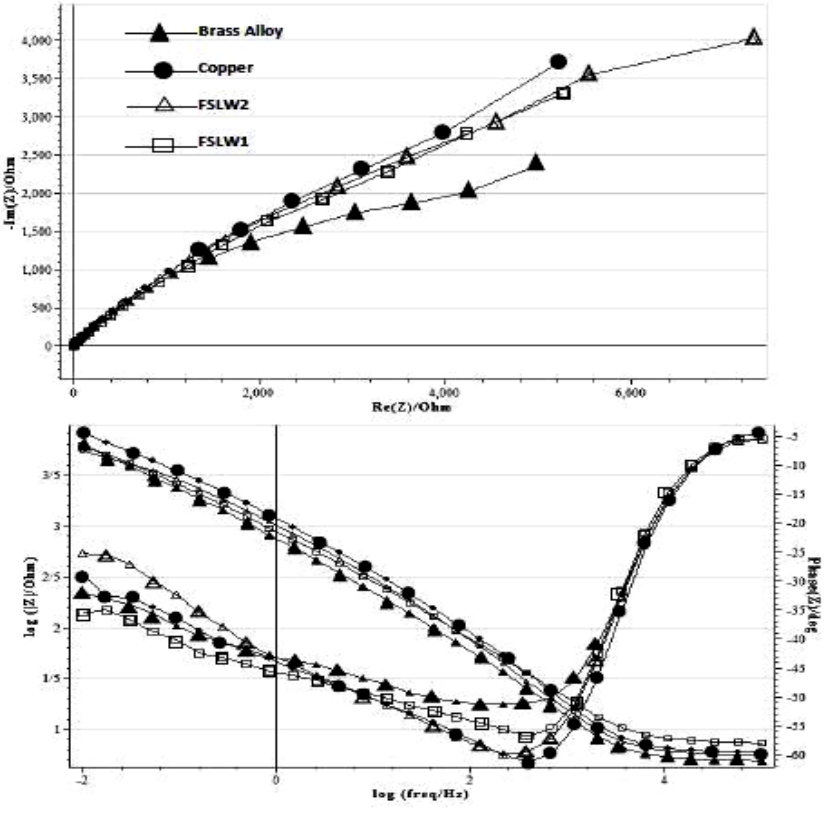

Fig. 7 The plots of (a): Nyquist and (b): Bode of Cu, brass alloy and welded copper/brass nugget zone in 1 M NaCl

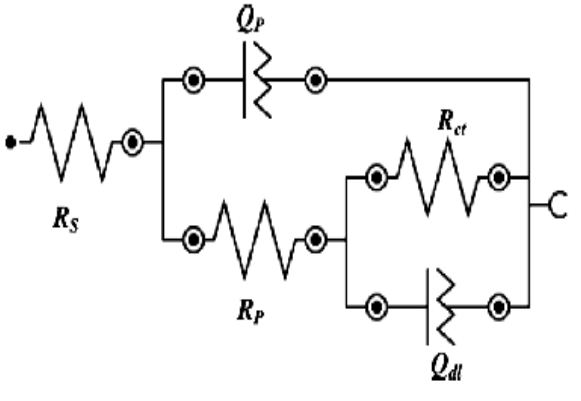

Fig. 8 Best equivalent circuit used for modeling experimental EIS data

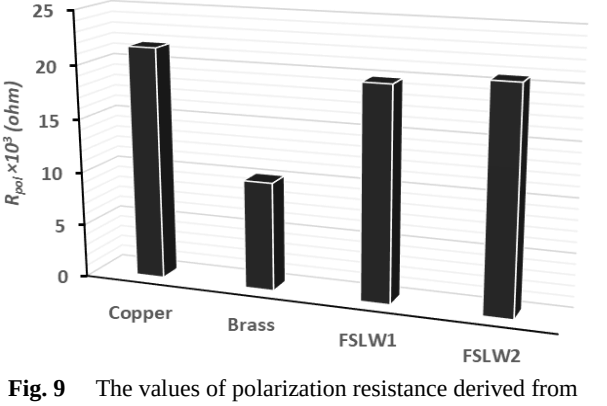

Fig. 9 The values of polarization resistance derived from modeling experimental EIS data for the Cu, brass and nugget zones formed at different welding heat inputs

This is consistent with pervious results from Nyquist curves as well. The nobler electrochemical behavior is known to be related to the modulus of impedance |Z|. Moreover, although the Bode plots do not conclude better electrochemical behavior for these examined specimens, the above-mentioned Nyquist plots implied a better function for pure copper sample than the previously confirmed. The results from EIS measurements suggest lower and higher corrosion resistance for welded regions compared to pure copper and brass metals, respectively. In this relation, the brass alloy has the lowest corrosion resistance rate.

3.4 *SEM* EXAMINATION *AFTER CORROSION*

Figure 10 shows SEM micrographs for welded sample surfaces formed in 1M NaCl solution after electrochemical tests. As seen in Fig. 10a, the welded sample surface has a high heat input during the welding process. A rough layer of corrosion products appeared to cover the surface, which was a cuprous dichloride complex ($CuCl_2^-$) or cuprite (Cu_2O). In fact, in a few spaces on the sample surface, the pit corrosion can be seen, as a local type of corrosion for copper and its alloys in 1M NaCl solution.

However, the welded sample surface with low heat input seems to be covered with a rough layer of corrosion products, alike the pervious sample, without a highlighted pit corrosion (Fig. 10b). Film formed on welded sample surface with a high heat input seems to be more porous in the film structure than the others. This oxide film is less protective. Hence, the oxide film leads to a diffusion-control corrosion process in both welded samples.

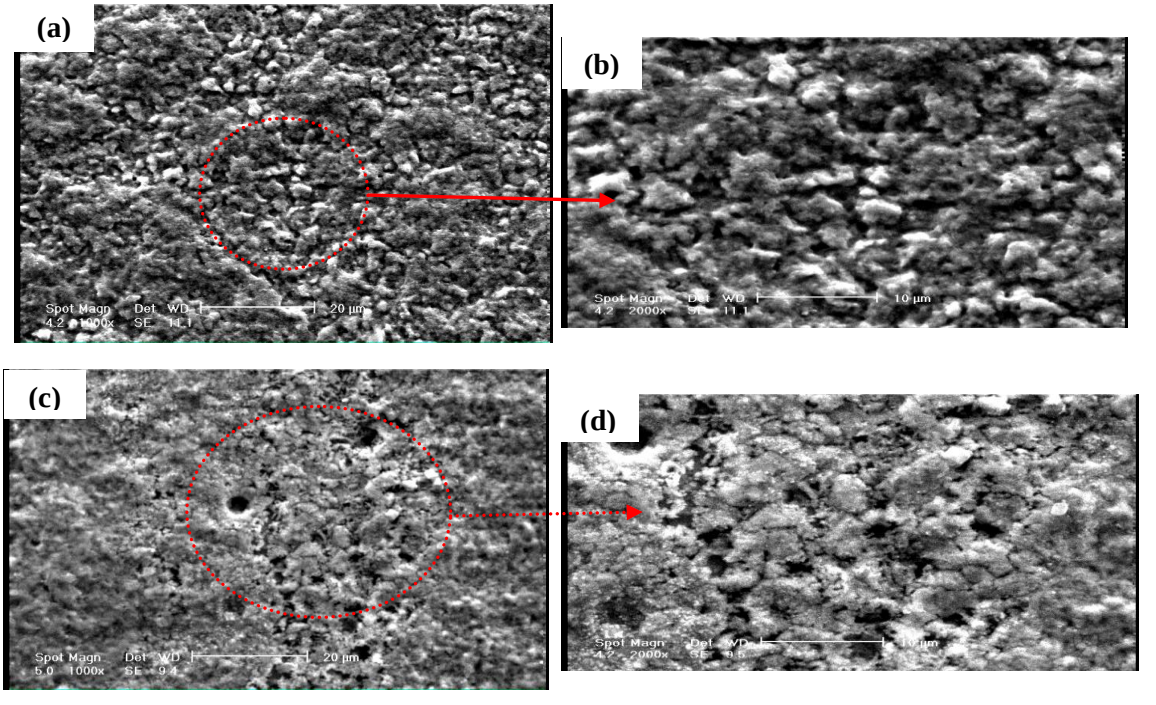

Fig. 10 The SEM micrographs of WNZ surfaces formed in the NaCl solution: (a, b): FSLW1 and (c, d): FSLW2

.

4 CONCLUSION

We investigated the Weld Nugget Zone electrochemical behavior of the Dissimilar Friction Stir Welded Lap Joints of Copper/Brass Metals in 1M NaCl solution (pH 7.2) via open circuit potential, potentio-dynamic polarization curves, and electrochemical impedance spectroscopy (EIS), and surface morphology studies. The study conclusions are as follows:

1- The open circuit potential measurements displayed reduced welded joints E_{ocp} with an increase in the heat input during the welding process, which had the lowest and highest values compared to copper and brass.

2- Tafel polarization curves showed an increase in the nugget zone I_{corr} of the welded joints with increasing the heat input due to intrinsic microstructural changes that occur during the welding process.

The results from EIS measurements presented the highest value for the polarization resistance for copper specimen, while the welded joints of NZ showed higher and lower values respectively than brass and copper.

3- The more porous oxide film formed on the welded joints NZ surface revealed an increase in the heat input during the welding process. This oxide film caused a diffusion- control corrosion process with less protection.

REFERENCES

[1] Cowie, J. G., Kundig, K. J. A., "Copper and Copper Alloys", In: Myer K (ed.) Handbook of Mechanical Engineers. Wiley Inter-Science., 2006, pp. 117- 220.

[2] Simonović, A. T., Radovanović, M. B., Petrović, M. B., Antonijević, M. M., and Milić, S. M., "Effect of Purine on Brass Behavior in the Neutral and Alkaline Sulphate Solutions", International Journal of Electrochemical Science, Vol. 7, 2012, pp. 11796 – 11810.

[3] Erdem M., "Examining the Structure and Mechanical Properties of Copper-Brass Plates Joined by Friction Stir Welding", International Journal of Advanced Manufacturing Technology, Vol. 76, 2015, pp. 1583–1592.

[4] Huang, Y. X., Dong, S. S., Zhou, L., Zhou, W. L., Feng, J.C., and He, W. X., "The Effect of Rotational Speed on the Microstructure and Mechanical Properties of Dissimilar Friction Stir-Welded Copper/Brass Metals", International Journal of Advanced Manufacturing Technology, DOI 10.1007/s00170-015-7792-9.

[5] Murch, M. G., Templesmith, P., Dawes, C. J., Thomas, W. M., Nicholas, E. D., and Need Ham, J. C., "Friction stir welding", International Patent Application, 1991, No. PCT/GB92102203 and GB Patent.

[6] Meran, C., "The Joint Properties of Brass Plates Caused by Friction Stir Welding", Material and Design., Vol. 27, 2006, pp. 719–726.

[7] Gharavi, F., Matori, K. A., Yunus, R., and Othman, N. K., "Study the Nugget Zone Corrosion Behavior in the Friction Stir Welded Lap Joints of 6061-T6 Aluminum Alloy", Mater. Rese., Vol. 17, No. 6, 2014, PP. 1563-1574.

[8] Amini, K., Gharavi, F., "The Impact of Welding Speed on the Corrosion Behavior of Friction Stir Welded AA5086 Aluminium Alloy", Journal of Central South University, Vol. 23, 2016, pp. 1301-1311.

[9] Tan, K. L., Hsieh, A. K., Feng, Y., Siow, K. S., and Teo, W. K., "The Copper Corrosion Mechanisms and Products of in Aqueous Solutions at Various pH Values", Corrosion., Vol. 53, No. 5, 1997, pp. 389-398.

[10] Ahmed, T. M., Tromans, D., and Alfantazi, A. M., "The Corrosion Behavior of Copper Alloys in Chloride Media", Mater. Des., Vol. 30, 2009, pp. 2425–2430.

[11] Kilincceker, G., Erbil, M., "The Effect of Phosphate Ions on the Electrochemical Behavior of Brass in Sulphate Solutions", Material Chemistry and Physics., Vol. 119, 2010, pp. 30–39.

[12] Burstein, G. T., "Tafel's Equation: One hundred years (1905–2005)", Corrosion Science, Vol. 47, 2005, pp. 2858.

[13] Tuthill, A. H., Todd, B., and Oldfield, J., "Study the Experiments with Copper Alloy Tubing Water Boxes and Pipes in the MSF Desalination Plants", International Congress on Desalination and Water Re-use, 1997, pp. 251-270.

[14] Griesss, J. C., Bacarella, A. L., "Anodic Dissolution of Cu in Flowing NaCl Solutions between 25 and 175 °C", Journal of Electrochemical Society, Vol. 120, 1973, pp. 459–65.

[15] Tromans, D., Silva, J. C., "Copper Behavior in Acidic Sulfate Solution: Compared with Acidic Chloride Solution, Corrosion, Vol. 53, 1997, pp. 171–8.

[16] Tromans, D., Sun, R., "Anodic Polarization Behavior of Copper in Aqueous Chloride/ Benzotriazole solutions, Journal of Electrochemical Society., Vol. 138, 1991, pp. 3235–55.

[17] Matthews, A., Liu, C., Bi, Q., and Leyland, A., "The Electrochemical Impedance Spectroscopic Study of the Corrosion Behavior of PVD Coated Steels in 0.5 N NaCl Aqueous Solution: Part I. Establishment of Equivalent Circuits for EIS Data Modeling, Corrosion Science, Vol. 45, 2003, pp. 1243–1256.